

Dose-Response: An International Journal

Volume 11 | Issue 2

Article 7

6-2013

COMPUTATIONAL MODELING OF CELLULAR EFFECTS POST-IRRADIATION WITH LOW- AND HIGH-LET PARTICLES AND DIFFERENT ABSORBED DOSES

Adriana Alexandre S. Tavares
Universidade do Porto, Portugal

João Manuel R. S. Tavares
Universidade do Porto, Portugal

Follow this and additional works at: https://scholarworks.umass.edu/dose_response

Recommended Citation

Tavares, Adriana Alexandre S. and Tavares, João Manuel R. S. (2013) "COMPUTATIONAL MODELING OF CELLULAR EFFECTS POST-IRRADIATION WITH LOW- AND HIGH-LET PARTICLES AND DIFFERENT ABSORBED DOSES," *Dose-Response: An International Journal*: Vol. 11 : Iss. 2 , Article 7.

Available at: https://scholarworks.umass.edu/dose_response/vol11/iss2/7

This Article is brought to you for free and open access by ScholarWorks@UMass Amherst. It has been accepted for inclusion in Dose-Response: An International Journal by an authorized editor of ScholarWorks@UMass Amherst. For more information, please contact scholarworks@library.umass.edu.

COMPUTATIONAL MODELING OF CELLULAR EFFECTS POST-IRRADIATION WITH LOW- AND HIGH-LET PARTICLES AND DIFFERENT ABSORBED DOSES

Adriana Alexandre S. Tavares and João Manuel R. S. Tavares □ Faculdade de Engenharia, Universidade do Porto, Portugal

□ The use of computational methods to improve the understanding of biological responses to various types of radiation is an approach where multiple parameters can be modelled and a variety of data is generated. This study compares cellular effects modelled for low absorbed doses against high absorbed doses. The authors hypothesized that low and high absorbed doses would contribute to cell killing via different mechanisms, potentially impacting on targeted tumour radiotherapy outcomes. Cellular kinetics following irradiation with selective low- and high-linear energy transfer (LET) particles were investigated using the Virtual Cell (VC) radiobiology algorithm. Two different cell types were assessed using the VC radiobiology algorithm: human fibroblasts and human crypt cells. The results showed that at lower doses (0.01 to 0.2 Gy), all radiation sources used were equally able to induce cell death ($p > 0.05$, ANOVA). On the other hand, at higher doses (1.0 to 8.0 Gy), the radiation response was LET and dose dependent ($p < 0.05$, ANOVA). The data obtained suggests that the computational methods used might provide some insight into the cellular effects following irradiation. The results also suggest that it may be necessary to re-evaluate cellular radiation-induced effects, particularly at low doses that could affect therapeutic effectiveness.

Keywords: computational methods, radiation-induced effects, cell kinetics, bystander effect, targeted tumour radiotherapy, Auger electrons, alpha particles, beta particles

1. INTRODUCTION

The Virtual Cell (VC) radiobiology simulator, was developed by Stewart and co-workers (Stewart 2004), to evaluate the following cellular endpoints: cell death, neoplastic transformation, chromosome aberration yields, induction of genomic instability, cell cycle kinetics and the probability of tumour eradication following radiation therapy. This simulator relies on multiscale modelling, which is essentially an integrative approach of multiple “sub-models” that are tested against measured data from *in vitro* systems. Thus, in order to model the emergent response of a group of cells or a tissue, these sub-models are linked together to form a “supermodel”. The postulated mechanisms, resulting from the multiscale supermodel, are subsequently compared to data from *in vivo* systems. This algorithm is an ongoing effort that aims to understand tumour pathogenesis and treatment; however, due to the complexity associated

Address correspondence to Prof. João Manuel R. S. Tavares, Faculdade de Engenharia, Universidade do Porto, Departamento de Engenharia Mecânica, Rua Dr. Roberto Frias, s/n, 4200-465 Porto, Portugal; Phone: +315 22 5081487; Fax: +315 22 5081445; Email: tavares@fe.up.pt; Url: www.fe.up.pt/~tavares

A. A. S. Tavares and J. M. R. S. Tavares

with such phenomena, simplified radiobiological models were used (Stewart 2004). Modelling cellular environments and cellular responses to irradiation by computational methods is complex and challenging. Radiation-induced effects are not yet fully understood, and regularly, new knowledge is added.

An important contribution from recent research to the field of cellular radiobiology was the evidence supporting the existence of radiation-induced bystander effects, i.e. effects detected in cells that were not directly “hit” by an ionizing radiation track (Boyd *et al.* 2006; Brooks 2004; Kassis 2003; Mother and Seymour 2003; Nagasawa *et al.* 2003; Persaud *et al.* 2005; Snyder 2004; Sokolov *et al.* 2005). Results from studies investigating radiation-induced bystander effects suggest that this effect will have implications on targeted radiotherapy microdosimetric estimates (Boswell and Brechbiel 2005; Britz-Cunningham and Adelstein. 2003; Kassis 2003) and on the current central radiobiological paradigm, where all radiation events are contained in the “hit” cell (Mother and Seymour 2003; Nagasawa *et al.* 2003). Multiple studies have found that radiation causes “hit” cells to produce signals that can be received by cells close or distant from the targeted cell, named recipient cells. In turn, these recipient cells transduce signals and coordinate a response, named adaptive response. Such coordinated response can be protective, for example, when an apoptotic response is initiated to remove abnormal cells from the population (Mother and Seymour 2006). Other intercellular mechanisms have also been described in the literature investigating the interplay between low doses of irradiation and intercellular induction of apoptosis. For example, work by Portess and Bauer in 2007 showed that transformed cells can be subject to reactive oxygen species-mediated apoptosis induction by non-transformed cells (Bauer 2007; Portess *et al.* 2007). All these responses do not seem to be dependent on the absorbed dose nor the radiation quality but appear to be dependent on genetic and environmental influences (Lyng *et al.* 2002; Mother and Seymour 2006; Snyder 2004; Sokolov *et al.* 2005). The multiple observations demonstrating that the bystander effects and the adaptive response are independent of radiation quality further reinforce the use of less conventional particles for targeted tumour radiotherapy, such as Auger electrons (Boswell and Brechbiel 2005; Boyd *et al.* 2006; Britz-Cunningham and Adelstein. 2003; Sofou 2008; Tavares and Tavares 2010a).

The cellular endpoints associated with the bystander effects include: mutation, gene induction, micronuclei formation, cell transformation and cell killing (Lyng *et al.* 2002; Mother and Seymour 2003; Nagasawa *et al.* 2003). These endpoints show a similar dose dependency, and therefore may be closely associated. In addition, bystander effects and genomic instability are both induced at very low doses, and there is evidence that bystander signals can induce genomic instability both *in vitro* and *in vivo*

Computational modeling of cellular effects post-irradiation

(Koturbash *et al.* 2006; Lyng *et al.* 2002; Mother and Seymour 2003). The authors hypothesized that the VC radiology simulator could be used to evaluate different cellular endpoints, including cell death and the induction of genetic instability, in order to investigate different aspects of cellular responses following irradiation. This paper aims to model cellular responses following irradiation with a wide range of absorbed doses and linear energy transfer (LET), in order to better understand the mechanisms that contribute to cell killing at low and high absorbed doses. Cell irradiation using Auger electrons, alpha particles and beta minus particles were modelled using the VC simulator and different irradiation scenarios.

2. METHODS

Previous studies have shown that the Technetium-99m (^{99m}Tc) CKMMX electron (all M-shell Coster-Kroning (CK) and super-CK transitions, $E = 1.16 \times 10^{-4}$ MeV) and Auger MXY (all M-shell Auger transitions, $E = 2.26 \times 10^{-4}$ MeV) could be classified as high LET particles, similar to Astatine-211 (^{211}At) alpha particles ($E = 6.79$ MeV) and in contrast to the Iodine-131 (^{131}I) beta minus particles ($E = 0.606$ MeV), which are low LET particles (Tavares *et al.* 2010b). Therefore, in this study the ^{99m}Tc CKMMX electrons and Auger MXY were used as high LET Auger emitters, the ^{211}At alpha particles as high LET alpha emitters and the ^{131}I beta minus particles as low LET emitters. The Monte Carlo damage simulation (MCDS) algorithm was used to obtain the number of double strand breaks (DSB) and the percentage of complex DSB (FCB) (Semenenko and Stewart 2005; Stewart 2004) for each investigated particle as previously reported (Tavares and Tavares 2010b). The MCDS simulator is a fast Monte Carlo algorithm that models the damages to DNA by different particles and captures the major trends in the DNA damage spectrum predicted using detailed track structure simulations (Semenenko and Stewart 2004). The results obtained from the MCDS simulator (DSB and FCB) that express the damage caused by the radioactive particle to the DNA per Gy per cell, were then applied as input parameters for the two-lesion kinetics (TLK) model used on the VC simulator. The approximate values of DSB and FCB obtained from the MCDS simulator for the evaluated particles were as follow: ^{99m}Tc CKMMX electrons DSB = 73.38 and FCB = 0.55; ^{99m}Tc Auger MXY DSB = 71.82 and FCB = 0.43; ^{211}At alpha particles DSB = 71.64 and FCB = 0.42; ^{131}I beta minus particles DSB = 40.89 and FCB = 0.13. By inserting these parameters, required by the TLK model, into the VC input file, the cellular exposure scenario modelled would mimic the isotope in close proximity to the cell nucleus. The TLK model was preferred over other radiation exposure models, such as the repair-misrepair model (RMR) and lethal-potentially lethal model (LPL), as it applies an improved correlation between the biochemical processes

A. A. S. Tavares and J. M. R. S. Tavares

of DSB and cell death, by subdividing DSB into simple or complex DSBs (Guerrero *et al.* 2002; Sachs *et al.* 1997; Stewart 2004; Tavares and Tavares 2010b).

A comprehensive list with all input parameters used on the VC simulations is presented in next section.

2.1 VC Simulator – Input Parameters

In this section only key VC input parameters used for the present study will be discussed, since an online platform, including a comprehensive VC user guide, is freely available on-line (<http://faculty.washington.edu/trawets/vc/ug/index.html>).

The cell kinetics model (CKM) used was the quasi-exponential cell kinetics model (QECK), as that is the only available option for the current version of the VC simulator. Nonetheless, by using a high peak cell density (KAP) value (such as the one used in the present study, i.e. $1.0E+38$ cells/cm³, Table 1) and by selecting a small initial cell population (initial number of cells – N0 = 1000 cells) compared to KAP×VOL (where VOL = tissue volume = 1 cm³, Table 1), the cell growth kinetics model becomes exponential. Furthermore, as the size of the cell population approaches KAP×VOL, the net cell birth rate decreases so that the cell population size approaches the asymptotic value KAP×VOL. The cell's DNA content at the G0 or G1 phase on the cell cycle and the number of chromosomes per cell (Table 1) were selected based on currently available biological knowledge of the human cell and human genome. Two different cell types were evaluated: 1) human fibroblasts (TPOT - cell doubling time=0.667 days = 16 hours) and 2) human intestinal crypt cells (TPOT=1.625 days = 39 hours) (Baserga 1971; Baserga 1993; Tavares and Tavares 2010b). The evaluated populations were set to be heterogeneous, with cycling and quiescent cells (GF – growth fraction=0.5), in order to mimic as close as possible the cellular biological reality *in vitro*, where dividing and quiescent cells coexist. The expected number of DSBs endogenously formed per cell-hour was set at $4.3349E-03$ Gy⁻¹ cell⁻¹ (Table 1). This value was chosen based on results from a study conducted by Stewart in 1999 (Stewart 1999).

The values of the biophysical parameters: repair half-time (RHT), pairwise damage interaction rate (ETA) and probability of correct repair (A0) were set according to the requisites of the selected damage repair model. For example, the TLK model used sets the RHT, ETA and A0 values at certain intervals, including those described in Table 1. The probability of misrejoined DSB being lethal (PHI) and the fraction of residual damage at the end of the simulation that is treated as lethal (FRDL) are adjustable parameters. The absolute residual damage cutoff (ACUT) value is also an adjustable parameter, and it terminates the simulation when the amount of unrepaired residual damage is less than the specified

*Computational modeling of cellular effects post-irradiation***TABLE 1.** Input conditions for VC simulator.

Summary of VC Key Input Conditions	References
<i>MODEL specification:</i>	
DRM (damage repair model)=TLK	(Stewart 2004)
CKM (cell kinetics model)=QECK (quasi-exponential cell kinetics model)	
<i>Cell parameters:</i>	
DNA (cell DNA content)=5.667E+09 base pair	(Stewart 2004)
NC (number of chromosomes per cell)=46	(Stewart 2004)
TPOT (cell doubling time)=0.667 or 1.625 days for fibroblasts and human crypt cells, respectively	(Baserga 1971; Baserga 1993)
GF (growth fraction, if 0 (zero) all cells are quiescent, if 1 (one) all cells are cycling and if 0.5 the cell population is heterogeneous)=0.5	N.A.
N0 (initial number of cells)=1000	N.A.
KAP (peak cell density)=1.0E+38 cells/cm ³	(Stewart 2004)
VOL (tissue volume)=1 cm ³	(Stewart 2004)
<i>Endogenous DNA damage parameters:</i>	
DSB (endogenous)=4.3349E-03 Gy-1 cell-1	(Stewart 2004)
<i>Biophysical parameters:</i>	
RHT (repair half-time)=XXX, XXX=0.25 9 h (simple DSBs are repaired faster than complex DSBs)	
ETA (pairwise damage interaction rate)=2.5E-04 h-1	
PHI (probability of a misrejoined DSB being lethal)=0.005	(Stewart 2004)
A0 (probability of correct repair)=AAA, AAA=0.95 0.25 (simple DSBs are repaired more accurately than complex DSBs)	
GAM (fraction of binary-misrepaired damages that are lethal)=0.25	
FRDL (fraction of residual that is lethal damage)=0.5	
<i>Key simulation stopping criterion:</i>	
ACUT (absolute residual-damage cutoff)=1.0E-09 expected number of DNA damages per cell	(Stewart 2004)
<i>Radiation exposure parameters:</i>	
BGDR (average background absorbed dose rate on planet Earth)=2.73748E-07 Gy/h	(UNSCEAR 2007) (Stewart 2004)
DCUT (dose cutoff used to truncate dose rate function after fraction 1-DCUT of total dose has been delivered)=0.01 Gy	
LAM (radioactive decay constant)=dependent on radionuclide used	N.A.
RHL (radionuclide half-life)=dependent on radionuclide used	N.A.
TCUT (time cutoff parameter)= 2 hours	N.A.
SAD (absorbed dose delivered in time interval 0-TCUT)=RX1, RX1=0.01 0.015 0.02 0.1 0.15 0.2 1 1.5 2 4 6 8 Gy	N.A.
STOL (step-size tolerance)=0.01 Gy/h	(Stewart 2004)

N.A. = not applicable.

value. Residual damages include radiation-induced DNA damages that remain unrepaired due to (1) DNA damage that was too severe, (2) presence of damages in inaccessible parts of the genome, (3) induction of damages during critical points in the cell cycle or (4) DNA damages converted into large DNA deletions (McMillan 1992). It is reasonable to accept that after a certain level of residual damages, any further cellular killing can be neglected as non-radiation related. The ACUT value of 1.0×10^{-9} expected number of DNA damages per cell was chosen based on the fact that it should be smaller than the spontaneous endogenous dam-

A. A. S. Tavares and J. M. R. S. Tavares

ages (established to be in the order of 10^{-3}) and a value of zero would not terminate the simulation, since ACUT was the only simulation control parameter adopted in the present study. The fraction of binary-misrepaired damages that are lethal (GAM) was set at 0.25 (Table 1), because according to Sach and co-workers (1997), around 1/4 of the chromosome aberrations formed through the pairwise interaction process are lethal (i.e., GAM=0.25) (Sachs *et al.* 1997).

The radiation exposure scenario selected was the exponentially decreasing dose rate (DECAY), since the present work aimed at modelling the cellular responses to different absorbed doses in a scenario of internal targeted radiotherapy using 3 radioisotopes (^{99m}Tc , ^{211}At and ^{131}I). For each radioisotope investigated, a radioactive constant (LAM) and a radionuclide half-life (RHL) was set according to the well known decay scheme of these radioisotopes. The average background absorbed dose rate on planet Earth (BGDR) has been quantified as 2.73748×10^{-7} Gy/h by the United Nations Scientific Committee on the Effects of Atomic Radiation (UNSCEAR) 2007 report (UNSCEAR 2007). Irradiation periods of 2 hours (TCUT, i.e. time cutoff parameter set at 2 hours) with total absorbed doses delivered to the cell population over all time (TAD) ranging between 0.01 and 8 Gy were modelled using the VC simulator. The effective dose delivered to the cell system in a finite time interval (0, TCUT), i.e. the SAD parameter is related to the TAD parameter by: $\text{SAD} = (1-\text{DCUT}) \times \text{TAD}$, where DCUT = the dose cutoff used to truncate dose rate function after fraction 1-DCUT of total dose has been delivered. The DCUT is an adjustable parameter of the VC simulator and in this study was set at 0.01, which means that the dose rate is truncated only after 99% of the set effective dose (SAD) has been delivered. This meant that $\text{SAD} \approx \text{TAD}$. The use of the DCUT parameter is justifiable since at a given point, the radioactivity of the radiation source becomes so small that any further radiation killing of the cell population can be neglected. The time to execute a DECAY simulation tends to increase as the number of steps increases. It is possible to control that by using the step-size tolerance (STOL) parameter, that typically ranges from about 0.05 to 1.0×10^{-3} Gy/h. As the STOL value decreases, the time requested to perform the simulation increases and thus, a compromise between time and accuracy must be made. In the present study, a STOL value of 0.01 Gy/h was used (Table 1).

A detailed description of the algorithm parameters used in the VC input file is given in Table 1.

2.2 Data analysis

The VC data was expressed as the number of direct lethal damages per surviving cell, estimated number of surviving cells, probability of mutagenesis and enhanced genetic instability per surviving cell, neoplas-

Computational modeling of cellular effects post-irradiation

tic transformation frequency per irradiated cell and neoplastic transformation frequency per surviving cell. In addition to analysis of the results including data from the whole range of the investigated absorbed doses, the results were also grouped as lower and higher absorbed doses. Since this paper is investigating the differences between cellular response to low and high absorbed doses, in the context of radiotherapy using particles, the cutoff value was set at 1.0 Gy. The lower doses were defined as those < 1.0 Gy, while higher doses were defined as doses ≥ 1.0 Gy. This criterion was based on previous findings showing that the cellular response to doses below 0.5 Gy would have a significant contribution from the bystander effect, while cellular response to doses above 0.5 Gy would behave as dose-dependent (Seymour and Mothersill 2000). Data differences among the investigated radioisotopes for the same absorbing doses were analysed using the ANOVA statistical test, where $p < 0.05$ was considered statically significant.

3. RESULTS

The estimated number of fibroblasts and crypt cells that survived irradiation when the cell population was heterogeneous (with quiescent cells and actively cycling cells) is presented in Figure 1(a) and 1(b), respectively. The results showed that the cell survival peaks at different doses, depending on the radioactive particle (^{99m}Tc electrons and ^{211}At alpha particles peak at around 0.15 and 0.2 Gy, while ^{131}I peaks at around 1.5 and 2.0 Gy). Statistical analysis revealed no differences among the results obtained for different particles, when the whole irradiation range was considered ($p = 0.77$, ANOVA). When dividing the evaluated dose range into lower irradiation doses (< 1.0 Gy) and higher irradiation doses (≥ 1.0 Gy), no statically significant differences were observable between distinct particles for lower doses ($p = 0.08$ for fibroblasts and $p = 0.19$ for crypt cells, ANOVA). However, statistically significant differences were seen for higher irradiation doses ($p = 0.03$ for fibroblasts and $p = 0.02$ for crypt cells, ANOVA).

Figure 2 shows the mutagenesis and enhanced genetic instability probability per surviving cell for different irradiating sources. Analysis of these curves reveals that the probability of mutagenesis and enhanced genetic instability of the cell population following irradiation with ^{99m}Tc selected electrons and ^{211}At alpha particles (high-LET particles) increased from 0 to 1.0 Gy, peaking at those absorbed dose levels and returning to negligible values at approximately 4.0 Gy. A curve peak shifting was observed for ^{131}I beta minus particles (low-LET particles) in comparison to the other irradiation sources. The highest probability of mutagenesis and enhanced genetic instability of the cell population following irradiation with ^{131}I beta minus particles was found at 4.0 Gy and negligible levels of mutagenesis and enhanced genetic instability post-peak were

A. A. S. Tavares and J. M. R. S. Tavares

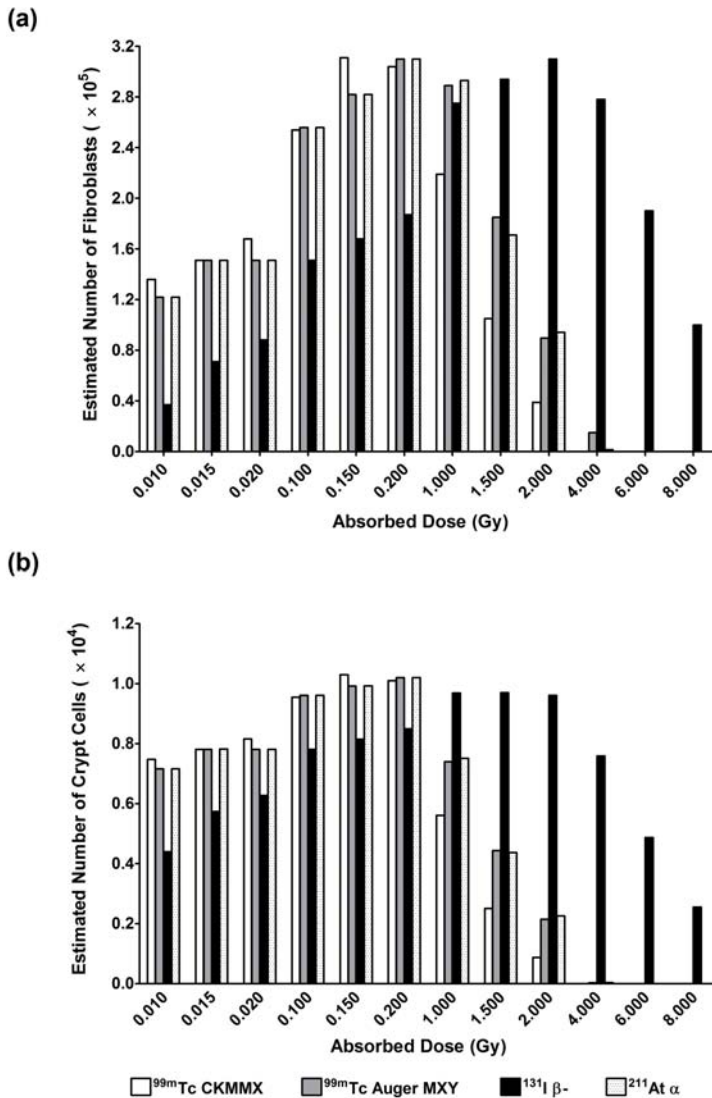


FIG. 1. Number of human fibroblasts (a) and human crypt cells (b) that survived irradiation with distinct particles (low- and high-LET particles) and different absorbed doses. Note the parabolic type relationship between absorbed dose and estimated number of surviving cells. Modelled conditions: time of radiation exposure = 2 hours, initial number of cells = 1000 and simulator stopping criterion for cell count following radiation exposure: ACUT=1.0D-09 expected number of DNA damages per cell.

not reached even at doses as high as 8.0 Gy. Statistical analysis of the whole dose range reveals no differences between the results obtained with the different investigated particles ($p=0.49$, ANOVA). However, when the duality lower dose/higher dose was taking into account (lower doses of <1.0 Gy; and higher doses of ≥ 1.0 Gy), statistically significant differences were found in each tail of the curves ($p=0.00$ for low doses and $p=0.04$ for high doses).

Computational modeling of cellular effects post-irradiation

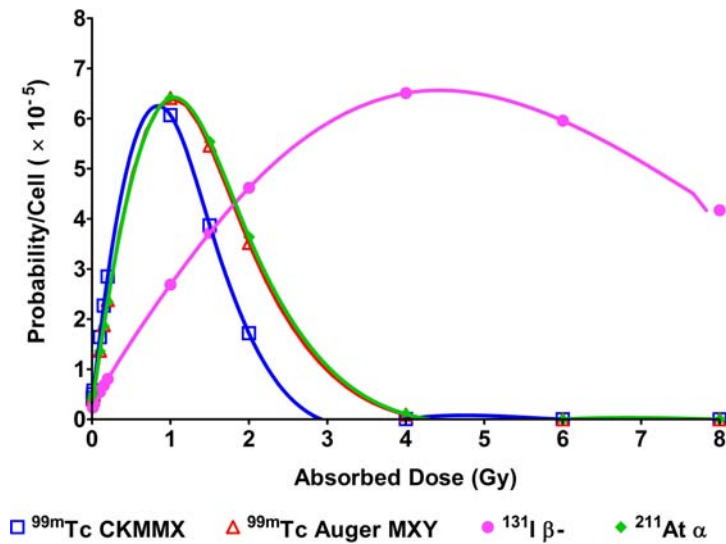


FIG. 2. Results from mutagenesis and enhanced genetic instability probability per surviving cell following exposure to different radiation sources and distinct absorbed doses. The probability per surviving cell following irradiation represents the probability of an altered gene function or expression causing enhanced genetic instability.

The neoplastic transformation frequency per irradiated cell and per surviving cell for each evaluated particle is shown in Figure 3a and 3b, respectively. The probability of neoplastic transformation per irradiated cell was highest for lower doses, regardless of the radioactive particle used, and reduced as the dose increased (Figure 3a). Conversely, the probability of neoplastic transformation frequency per surviving cell was lowest for low absorbed doses and increased as the absorbed dose increased (Figure 3b). The reduction rates of neoplastic transformation frequency per irradiated cell varied for low- and high-LET particles, where the steepest reduction was observed for high-LET particles, and a slower reduction was found for low-LET particles. Statistically significant differences were observed among distinct radioactive particle neoplastic transformation frequencies per irradiated cell ($p=0.00$, ANOVA). In a similar manner, the increase rate of neoplastic transformation frequency per surviving cell varied for low- and high-LET particles, where the steepest increase was observed for high-LET particles, and a slower increase was determined for low-LET particles ($p=0.00$, ANOVA).

Finally, Figure 4 shows the number of direct lethal damages per surviving cell as a function of absorbed dose. The results showed a rapid increase in cellular lethal damages as the absorbed dose increased, and statistically significant differences were observed among the results using distinct particles ($p=0.00$, ANOVA).

A. A. S. Tavares and J. M. R. S. Tavares

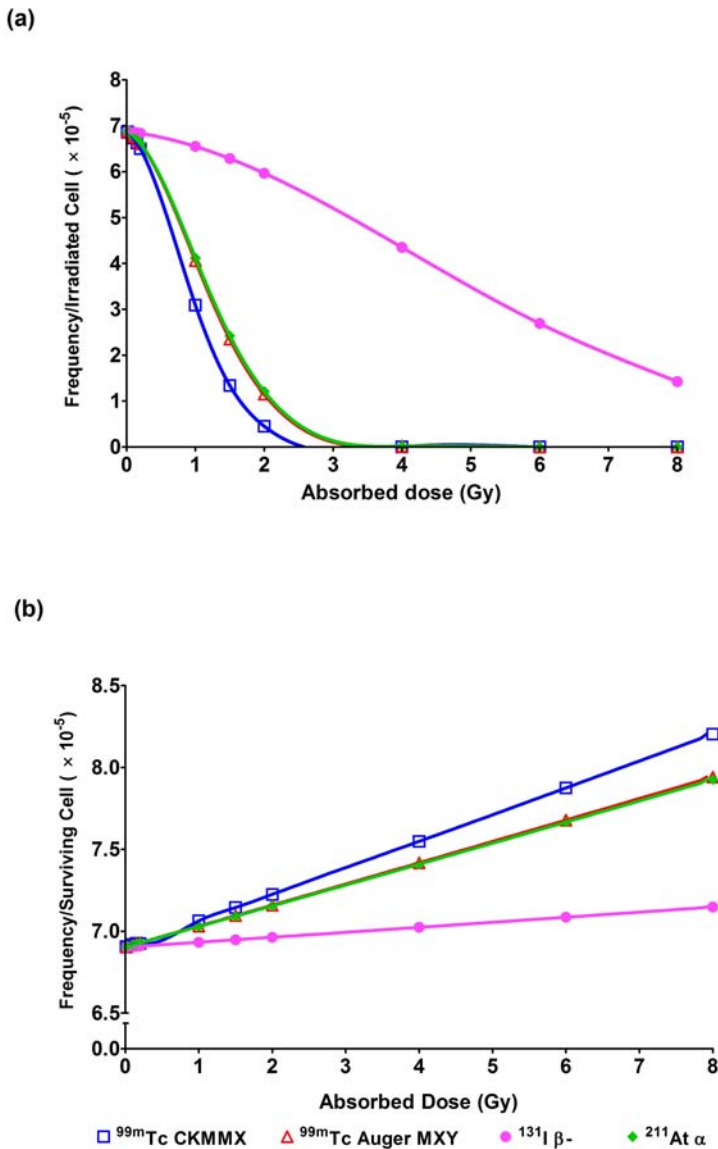


FIG. 3. Neoplastic transformation frequency per irradiated cell (a) and per surviving cell (b), expressed in week^{-1} , following exposure to different radiation sources and distinct absorbed doses.

4. DISCUSSION

The results showed that the estimated number of surviving cells increased, peaked and decreased as a function of absorbed dose, describing a non-linear parabolic-type curve (Figure 1). No differences were found among the results using distinct particles for lower absorbed doses, but differences were observed at higher absorbed doses. The absence of differences among results with distinct particles for lower doses, suggests

Computational modeling of cellular effects post-irradiation

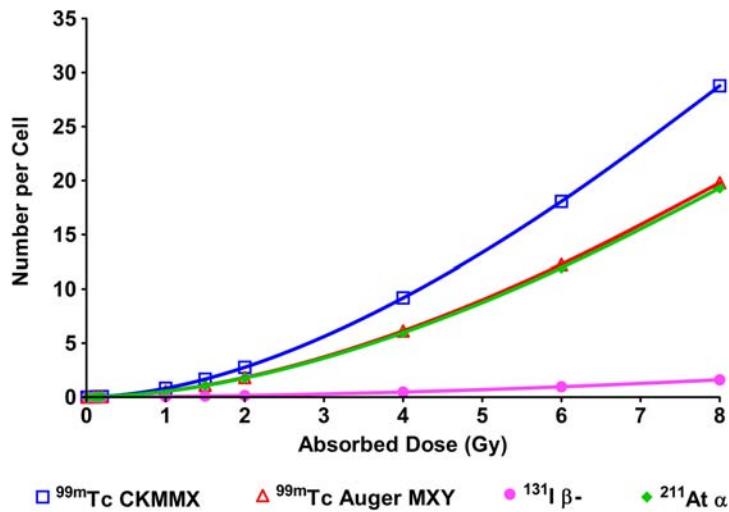


FIG. 4. Average number of direct lethal damages per surviving cell after irradiation with distinct particles and different absorbed doses. Note the rapid increase in the number of lethal mutations per cell as a function of absorbed dose and different cellular dose-response curves depending on particle LET.

that another factor, other than radiation quality, may be responsible for the inexistence of differences among the particles. Conversely, at higher doses, the cell response appears to behave in a LET and dose dependent manner. To further clarify the nature of the non-linear curve following irradiation of human fibroblasts and human crypt cells with different particles, three cellular endpoints were assessed by computational simulation: mutagenesis and enhanced genetic instability per surviving cell (Figure 2), neoplastic transformation per irradiated or surviving cell (Figure 3) and number of direct lethal damages per surviving cell (Figure 4).

Mutagenesis and enhanced genetic instability results showed that there is a non-linear relationship between genomic instability and absorbed dose (Figure 2), which is in agreement with previous observations (Mother and Seymour 2003; Seymour and Mothersill 2000). Sokolov and co-workers in 2005, using primary human fibroblasts, found that for doses of alpha particles and gamma rays between 0.2 and 0.6 Gy, the number of DSB sites in bystander cells was higher than for doses of 2.0 Gy (Sokolov *et al.* 2005). DNA DSBs have been associated with genetic instability, which is one of the mechanisms underlying the bystander effect. The results from the VC simulator showed that the probability of mutagenesis and genetic instability for alpha particles (and the other high LET particles investigated) was higher for doses ranging between 0.2 and 1.5 Gy than for doses equal to or above 2.0 Gy (Figure 2). These findings seem to be in line with *in vitro* observations reported by Sokolov and co-workers in 2005 (Sokolov *et al.* 2005).

A. A. S. Tavares and J. M. R. S. Tavares

The data also showed that probability of cell transformation per irradiated cell was higher for lower absorbed doses (Figure 3a), while the probability of cell transformation per surviving cell (Figure 3b) and the number of direct lethal damages per surviving cell (Figure 4) was higher for high absorbed doses. Redpath and co-workers studies have also reported that the cell transformation frequency per surviving cell increased with increasing absorbed doses (Pant *et al.* 2003; Redpath 2006; Redpath and Elmore 2007). Other studies have found that as the absorbed dose increased, the direct damage component of cellular response to radiation increased, and at doses above 0.1-0.4 Gy the direct damage component was the main contributor responsible for the cellular response to irradiation (Brenner *et al.* 2001; Leonard 2008). Results from the VC simulator are in line with these prior observations. The increasing probability of cell transformation per surviving cell with increasing absorbed doses means that the normal cells surrounding the tumour have to be protected when performing target tumour radiotherapy, particularly for high doses of radiation.

Taken all together, these data show that, at the lower absorbed doses, the genetic instability of surviving cells and the transformation frequency per irradiated cell are the two major contributors for the low number of estimated surviving cells, since the values of direct lethal damages and transformation frequency per surviving cell for lower doses are small compared with higher absorbed doses. Conversely, at higher absorbed doses, cell death is mainly related to the number of direct lethal damages, the transformation frequency per surviving cell and the radiation quality. This does not mean that genetic instability of surviving cells and transformation frequency per irradiated cell effects have no relevance at higher doses but that their relative importance as a portion of the total effect tends to decrease as the dose increases. Previous studies have pointed out similar conclusions (Mother and Seymour 2003; Seymour and Mothersill 2000) providing confidence in this model and the results obtained here. Another study by Liu and co-workers in 2007, using computational models and HPV-G human skin keratinocytes exposed to gamma rays, found that for doses above 0.3 to 0.5 Gy, the survival response of the bystander cells reached a plateau, suggesting that the emission of bystander signals may be saturated at that point (Liu *et al.* 2007). This would mean that for doses above 0.3 to 0.5 Gy, the cellular response to radiation will be mainly dependent on direct radiation effects rather than on bystander effects, such as, genetic instability and irradiated cell transformation (Koturbash *et al.* 2006; Lyng *et al.* 2002; Mother and Seymour 2003). The experimental scenarios modelled by Liu and co-workers, that were validated using *in vitro* medium transfer experiments (Liu *et al.* 2007), agree with the results using the VC simulator, which further provide confidence in the simulator used in this paper. An interpretation of the low number of surviving

Computational modeling of cellular effects post-irradiation

cells obtained for lower absorbed doses could be the protective adaptive response, where the genetic instability in surviving cells and the neoplastic transformation of irradiated cells would result in a triggering of the apoptotic response to eliminate damaged cells from the population. This type of adaptive response can be classified as a positive outcome of the bystander effects (Leonard 2008; Mother and Seymour 2006).

Given the close links found between genetic instability, cell transformation and the bystander effect (Koturbash *et al.* 2006; Lyng *et al.* 2002; Mother and Seymour 2003), the VC simulator might be useful as a first line screening tool for prediction and modelling of cellular effects and possibly the bystander effects at lower absorbed doses. Although this cannot be taken as granted without *in vitro* studies performed under the same conditions as those modelled in the VC simulator. The data obtained from the VC simulator should be interpreted with caution due to the parameter estimation issues associated with mechanism-based radiation response models. Although flexibility in changing input parameters will have obvious advantages by allowing the modelling of multiple irradiation scenarios, it also represents an issue due to the uncertainty associated with the choice of a certain value in detriment of another. Sensitivity testing of the model control parameters may provide more confidence to use the simulator by adding error bars to the data collected. Together with *in vitro* or *in vivo* studies data, the simulators such as the one presented in this work, would allow better experimental design and could be used to study different processes associated with cell response to ionizing radiation. Thus, future *in vitro* and *in vivo* studies are crucial to establish a definite role of the simulator used here and careful interpretation of the results is therefore recommended. Another important consideration regarding the use of models for studying cellular effects of low doses of radiation is the fact that radiobiology models do not accommodate new findings. This means that future research may deem the VC simulator useful or obsolete. In addition, as long as the mechanisms of radiation induced cellular effects for low absorbed doses remain unclear, modelling low dose effects is difficult and uncertainty is high. In fact, the identification of models to better quantify the cellular response to low doses of radiation is one of the key challenges facing the radiation research community (Stewart *et al.* 2006). Nevertheless, the comparative analysis of the VC generated data with prior studies (discussed above), support the use of the VC simulator as a useful tool in the field of radiobiology, with particular interest in the context of radiotherapy. Several other mathematical models have been proposed to quantify the impact of low absorbed doses on the dose-response curves for ionizing radiation (Brenner *et al.* 2001; Fornalski *et al.* 2011; Leonard 2008; Little *et al.* 2005; Nikjoo and Khvostumov 2003).

A. A. S. Tavares and J. M. R. S. Tavares

In this paper, the use of computational methods to model an internal radiotherapy scenario, where the radioisotope is inserted close to the cell nucleus, was investigated. This is of key importance in targeted tumour radiotherapy, because if the radioisotope was decaying outside the cell or in the cell cytoplasm, the outcome would be different, as shown in previous studies investigating the relationship between the decay site distance to the cell nucleus and the energy deposition into the DNA molecule (Boyd *et al.* 2006; Humm *et al.* 1994; Tavares and Tavares 2010a). Under the modelled scenario here, the work contributes to the current literature on targeted radiotherapy by pin-pointing that cellular effects at low doses can be an important contribution for microdosimetric estimations and may impact the therapeutic effectiveness prediction. Furthermore, the findings further support the current view that the overall “target” population after irradiation exposure at lower doses might be larger than that predicted using the traditional dosimetric methods. The results using the VC simulator suggest that targeted tumour radiotherapy with low absorbed doses might be as efficient in cell killing as very high absorbed doses, despite the cell mechanisms associated with each side of the dose-response curve (low *versus* high absorbed doses) being considerably different. This study focused on targeted tumour radiotherapy scenarios, where the radioactive source was inserted near the cell nucleus. The radioisotopes studied included beta emitters, Auger electrons emitters and alpha emitters, covering the most commonly used particles in current targeted tumour radiotherapy. Doses ranging 1 cGy and 8.0 Gy were tested on heterogeneous cell populations and the number of surviving cells following irradiation was estimated. Nonetheless, if the purpose was to investigate cellular response in the context of domestic or occupational exposure to ionizing radiation, i.e. radiation protection studies, the exposure scenarios would have to be modelled in a different manner. Both targeted tumour radiotherapy studies and radiation protection studies can be modelled using the VC simulator by altering the input conditions, such as the number of DSB and fraction of complex DSB, the damage-repair model or other parameters. The VC simulator is a user friendly platform that provides output data consistent with experimental terminology used by cellular radiobiologists. This might foster the future use of the VC simulator by non-computer scientists, by using a similar approach as the one described here.

In conclusion, data obtained using the VC simulator indicate that low doses of all tested particles (^{99m}Tc Auger electrons, ^{211}At alpha particles and ^{131}I beta minus particles) seem to be equally able to induce cell death independently of their LET. At low doses cell death was found to be due to high genetic instability and cell transformation that are cellular endpoints measured when investigating the bystander effect. On the contrary, at high absorbed doses, cellular response to radiation seems to be

Computational modeling of cellular effects post-irradiation

dose and LET dependent. These findings can impact targeted tumour radiotherapy outcome predictions and suggest that the traditional radiobiological paradigm of radiation-induced effects contained in the “hit” cell may be obsolete. In addition, the data here suggest that the use of novel therapeutic approaches with unconventional types of radioisotopes may hold promise for targeted tumour radiotherapy.

ACKNOWLEDGEMENTS

The authors wish to thank Dr Robert Stewart (School of Health Sciences – Purdue University, USA) for providing the simulator software package used and for his kind technical assistance.

REFERENCES

- Baserga R. 1971. The Cell Cycle and Cancer. In: Farber E (ed), *The Biochemistry of Disease - A Molecular Approach to Cell Pathology - Volume I*, pp. 22. Marcel Dekker, USA
- Baserga R. 1993. Defining the Cycle. In: Sadava D (ed), *Cell Biology - Organelle Structure and Function*, pp. Jone and Barlett Publishers, USA
- Bauer G. 2007. Low dose radiation and intercellular induction of apoptosis: potential implications for the control of oncogenesis. *Int J, Rad Biol* 83:873-888
- Boswell C and Brechbiel M. 2005. Auger Electrons: Lethal, Low Energy, and Coming Soon to a Tumor Cell Nucleus Near You. *J Nucl Med* 46:1946-1947
- Boyd M, Ross S, Dorrens J, Fullerton N, Tan K, Zalutsky M and Mairs R. 2006. Radiation-Induced Biologic Bystander Effect Elicited In Vitro by Targeted Radiopharmaceuticals Labeled with α -, β - and Auger Electrons-Emitting Radionuclides. *J Nucl Med* 47:1007-1015
- Brenner D, Little J and Sachs R. 2001. The Bystander Effect in Radiation Oncogenesis: II. A Quantitative Model. *Radiat Res* 155:402-408
- Britz-Cunningham S and Adelstein J. 2003. Molecular Targeting with Radionuclides: State of the Science. *J Nucl Med* 44:1945-1961
- Brooks AL. 2004. Evidence for “bystander effects” *in vivo*. *Hum Exp Toxicol* 23:67-70
- Fornalski KW, Dobrzynski L and Janiak MK. 2011. A Stochastic Markov Model of Cellular Response to Radiation. *Dose-Response* 9:477-496
- Guerrero M, Stewart R, Wang J and Li X. 2002. Equivalence of linear-quadratic and two-lesion kinetic models. *Phys Med Biol* 47:3197-3209
- Humm J, Howell R and Rao D. 1994. Dosimetry of Auger-Electron-Emitting Radionuclides. *Med Phys* 21:1901-1915
- Kassis A. 2003. Cancer Therapy with Auger Electrons: Are We Almost There? *J Nucl Med* 44:1479-1481
- Koturbash I, Rugo RE, Hendricks CA, Loree J, Thibault B, Kutanzi K, Pogribny I, Yanch JC, Engelward BP and Kovalchuk O. 2006. Irradiation induced DNA damage and modulates epigenetic effectors in distant bystander tissue *in vivo*. *Oncogene* 25:4267-4275
- Leonard B. 2008. A Review: Development of a Microdose Model for Analysis of Adaptive Response and Bystander Dose Response Behavior *Dose-Response* 6:113-183
- Little M, Filipe J, Prise KM, Folkard M and Belyakov O. 2005. A model for radiation-induced bystander effects, with allowance for spatial position and the effects of cell turnover. *J Theor Biol* 232:329-338
- Liu Z, Prestwich W, Stewart R, Byun S, Mothersill C, McNeill F and Seymour C. 2007. Effective Target Size for the Induction of Bystander Effects in Medium Transfer Experiments. *Radiat Res* 168:627-630
- Lyng FM, Seymour C and Mothersill C. 2002. Early Events in the Apoptotic Cascade Initiated in Cells Treated with Medium from the Progeny of Irradiated Cells. *Radiat Prot Dosimetry* 99:169-172
- McMillan T. 1992. Residual DNA damage: what is left over and how does this determine cell fate? *Eur J Cancer* 28:267-269

A. A. S. Tavares and J. M. R. S. Tavares

- Mothersill C and Seymour C. 2003. Radiation-induced bystander effects, carcinogenesis and models. *Oncogene* 22:7028-7033
- Mothersill C and Seymour C. 2006. Radiation-induced bystander effects: evidence for an adaptive response to low dose exposures? *Dose-Response* 4:283-290
- Nagasawa H, Huo L and Little J. 2003. Increased bystander mutagenic effect in DNA double-strand break repair-deficient mammalian cells. *Int J Radiat Biol* 79:35-41
- Nikjoo H and Khvostumov I. 2003. Biophysical model of the radiation-induced bystander effect. *Int J, Rad Biol* 79:43-52
- Pant MC, Liao X-Y, Lu Q, Molloy S, Elmore E and Redpath JL. 2003. Mechanisms of suppression of neoplastic transformation in vitro by low doses of low LET radiation. *Carcinogenesis* 24:1961-1965
- Persaud R, Zhou H, Baker SE, Hei TK and Hall EJ. 2005. Assessment of Low Linear Energy Transfer Radiation-Induced Bystander Mutagenesis in a Three-Dimensional Culture Model. *Cancer Res* 65:9876-9882
- Portess D, Bauer G, Hill M and O'Neill P. 2007. Low-Dose Irradiation of Nontransformed Cells Stimulates the Selective Removal of Precancerous Cells via Intercellular Induction of Apoptosis. *Cancer Res* 67:1246-1253
- Redpath JL. 2006. Suppression of neoplastic transformation in vitro by low doses of low LET radiation. *Dose-Response* 4:302-308
- Redpath JL and Elmore E. 2007. Radiation-induced neoplastic transformation in vitro, hormesis and risk assessment. *Dose-Response* 5:123-130
- Sachs R, Hahnfeld P and Brenner D. 1997. The link between low-LET dose-response relations and the underlying kinetics of damage production/repair/misrepair. *Int J Radiat Biol* 72:351-374
- Semenenko V and Stewart R. 2004. A Fast Monte Carlo Algorithm to Simulate the Spectrum of DNA Damages Formed by Ionizing Radiation. *Radiat Res* 161:451-457
- Semenenko V, Stewart R and Ackerman E. 2005. Monte Carlo Simulation of Base and Nucleotide Excision Repair of Clustered DNA Damage Sites. I. Model Properties and Predicted Trends. *Radiat Res* 164:180-193
- Seymour C and Mothersill C. 2000. Relative Contribution of Bystander and Targeted Cell Killing to the Low-Dose Region of the Radiation Dose-Response Curve. *Radiat Res* 153:508-511
- Snyder AR. 2004. Review of radiation-induced bystander effects. *Hum Exp Toxicol* 23:87-89
- Sofou S. 2008. Radionuclide carriers for targeting of cancer. *Int J Nanomedicine* 3:181-199
- Sokolov MV, Smilenov LB, Hall EJ, Panyutin IG, Bonner WM and Sedelnikova OA. 2005. Ionizing radiation induces DNA double-strand breaks in bystander primary human fibroblasts. *Oncogene* 24:7257-7265
- Stewart R. 1999. On the complexity of the DNA damages created by endogenous process. *Radiat Res* 152:101-104
- Stewart R. 2004. VC Simulator (Virtual Cell Radiobiology Simulator), Resources for information on VC simulator package. Available at <http://faculty.washington.edu/trawets/vc/index.html>
- Stewart R, Ratnayake R and Jennings K. 2006. Microdosimetric Model for the Induction of Cell Killing through Medium-Borne Signals. *Radiat Res* 165:460-469
- Tavares A and Tavares J. 2010a. ^{99m}Tc Auger Electrons for Targeted Tumour Therapy: A Review. *Int J Radiat Biol* 86:261-270
- Tavares A and Tavares J. 2010b. Evaluating ^{99m}Tc Auger Electrons for Targeted Tumor Radiotherapy by Computational Methods. *Med Phys* 37:3551-3559
- UNSCEAR. 2007. Report of the United Nations Scientific Committee on the Effects of Atomic Radiation to the General Assembly, Vienna, Austria